Soil Biology & Biochemistry 43 (2011) 2315–2323

Contents lists available at SciVerse ScienceDirect

Soil Biology & Biochemistry

journal homepage: www.elsevier.com/locate/soilbio

The magnitude and variability of soil-surface CO_2 efflux increase with mean annual temperature in Hawaiian tropical montane wet forests

Creighton M. Litton [a,*], Christian P. Giardina [b], Jeremy K. Albano [a], Michael S. Long [a], Gregory P. Asner [c]

[a] Department of Natural Resources and Environmental Management, University of Hawaii at Manoa, 1910 East West Rd., Honolulu, HI 96822, USA
[b] USDA Forest Service, Institute of Pacific Islands Forestry, Pacific Southwest Research Station, 60 Nowelo St., Hilo, HI 96720, USA
[c] Department of Global Ecology, Carnegie Institution, 260 Panama Street, Stanford, CA 94305, USA

ARTICLE INFO

Article history:
Received 12 March 2011
Received in revised form
8 August 2011
Accepted 9 August 2011
Available online 24 August 2011

Keywords:
Hawaii
Mean annual temperature (MAT)
Soil-surface CO_2 efflux – 'soil respiration' – F_S
Spatial and diel variability
Tropical montane wet forests

ABSTRACT

Soil-surface CO_2 efflux (F_S; 'soil respiration') accounts for ≥50% of the CO_2 released annually by the terrestrial biosphere to the atmosphere, and the magnitude and variability of this flux are likely to be sensitive to climate change. We measured F_S in nine permanent plots along a 5.2 °C mean annual temperature (MAT) gradient (13–18.2 °C) in Hawaiian tropical montane wet forests where substrate type and age, soil type, soil water balance, disturbance history, and canopy vegetation are constant. The objectives of this study were to quantify how the (*i*) magnitude, (*ii*) plot-level spatial variability, and (*iii*) plot-level diel variability of F_S vary with MAT. To address the first objective, annual F_S budgets were constructed by measuring instantaneous F_S monthly in all plots for one year. For the second objective, we compared plot-level mean instantaneous F_S in six plots derived from 8 versus 16 measurements, and conducted a power analysis to determine adequate sample sizes. For the third objective, we measured instantaneous F_S hourly for 24 h in three plots (cool, intermediate and warm MATs). The magnitude of annual F_S and the spatial variability of plot-level instantaneous F_S increased linearly with MAT, likely due to concomitant increases in stand productivity. Mean plot-level instantaneous F_S from 8 versus 16 measurements per plot yielded statistically similar patterns. The number of samples required to estimate plot-level instantaneous F_S within 10% and 20% of the actual mean increased with MAT. In two of three plots examined, diel variability in instantaneous F_S was significantly correlated with soil temperature but minimal diel fluctuations in soil temperature (<0.6 °C) resulted in minimal diel variability in F_S. Our results suggest that as MAT increases in tropical montane wet forests, F_S will increase and become more spatially variable if ecosystem characteristics and functioning undergo concurrent changes as measured along this gradient. However, diel variation in F_S will remain a minor component of overall plot-level variation.

1. Introduction

In terrestrial ecosystems, soil-surface CO_2 efflux (F_S; 'soil respiration') is derived primarily from belowground autotrophic and heterotrophic metabolism, and to a lesser degree from the dissolution of carbonates and photodegradation of organic matter (Kuzyakov, 2006; Vargas et al., 2011). The annual release of CO_2 from soils to the atmosphere as F_S follows gross primary production (GPP) as the second largest carbon (C) flux in the global terrestrial C cycle (Raich and Schlesinger, 1992). At the stand scale, F_S in forest ecosystems can account for 50% or more of GPP and 70% or more of total ecosystem respiration (Janssens et al., 2001; Khomik et al., 2010; Law et al., 1999). At the global scale, F_S in tropical broadleaf forests accounts for ~30% of the global annual F_S budget (Raich et al., 2002).

Because F_S typically increases with temperature, especially in the absence of moisture limitations, future warming is anticipated to impact terrestrial C cycling and atmospheric CO_2 concentrations (Bond-Lamberty and Thomson, 2010; Litton and Giardina, 2008). Warming-related increases in F_S have been documented both during spring warming (Boone et al., 1998; Davidson et al., 1998) and across gradients of mean annual temperature (MAT) (Rodeghiero and Cescatti, 2005; Townsend et al., 1995; Zimmermann et al., 2010). While these prior studies yield important insights into large-scale patterns, variables other than temperature can strongly influence F_S and these often vary temporally with spring warming studies (e.g., fine root biomass,

* Corresponding author. Tel.: +1 808 956 6004; fax: +1 808 956 6539.
E-mail addresses: litton@hawaii.edu (C.M. Litton), cgiardina@fs.fed.us (C.P. Giardina), gpa@stanford.edu (G.P. Asner).

0038-0717/$ – see front matter © 2011 Elsevier Ltd. All rights reserved.
doi:10.1016/j.soilbio.2011.08.004

photosynthetically active radiation, and canopy mass) or spatially with MAT gradient studies (e.g., substrate and soil type, precipitation, vegetation composition, disturbance history). Despite these potentially confounding variables, these studies are often interpreted to mean that future warming will accelerate heterotrophic losses of belowground organic C pools and result in a positive feedback between F_S and global climate change. Alternatively, because total belowground C flux (TBCF) increases with MAT (Litton and Giardina, 2008), an increase in F_S with warming may result from an increased supply of belowground substrate with no change in soil C storage and no positive feedback on climate (Bond-Lamberty and Thomson, 2010). This is a topic of considerable importance to understanding feedbacks between global climate change and terrestrial C cycling.

Regardless of the mechanism driving changes in F_S with temperature, representative field estimates of F_S at the plot level are needed to accurately model terrestrial ecosystem metabolism (Vargas et al., 2011). F_S integrates belowground processes and constrains C budgets (Ryan and Law, 2005), which in turn are needed to better understand belowground (Davidson et al., 2006; Tang et al., 2005) and ecosystem (Urbanski et al., 2007) respiratory responses to warming. An obstacle to achieving representative field estimates of F_S, however, is its inherent spatial and temporal variability (Adachi et al., 2005; Katayama et al., 2009; Stoyan et al., 2000). While the various environmental controls on F_S have been investigated extensively (e.g., temperature, moisture, plant activity, litterfall, soil organic matter) (Kuzyakov, 2006; Ryan and Law, 2005; Vargas et al., 2011), the factors influencing spatial and temporal variability in F_S remain poorly understood (Fang et al., 1998; Rodeghiero and Cescatti, 2008), particularly in tropical forests (Katayama et al., 2009). Yet accurate estimates of F_S in forest stands must incorporate spatial and temporal variability when scaling from instantaneous point measurements to monthly or yearly stand budgets (Vargas et al., 2011), which are arguably the most meaningful scales for understanding and modeling ecosystem metabolism.

Hawaii supports several important model ecological systems for understanding the response of terrestrial biogeochemistry to biophysical parameters, notably substrate age, precipitation and temperature (Vitousek, 2004). For this study, we established a highly controlled, 5.2 °C (13–18.2 °C) MAT gradient spanning 800 m elevation (800–1600 m.a.s.l.) in native tropical montane wet forests on the windward side of the Island of Hawaii. This gradient provides an ideal system for addressing globally relevant questions regarding the response of terrestrial C cycling, including F_S, to rising temperature because other environmental drivers of C dynamics such as soil water balance, substrate type and age, soil type, canopy vegetation composition, and disturbance history are largely constant across the gradient. While past model projections of climate change in the tropics, particularly on tropical islands, predicted only small increases in temperature with global climate change, surface temperatures over the past ~30 years in Hawaii at elevations >800 m have risen at a rate (0.268 °C decade^{-1}) comparable to, or exceeding, global trends (Giambelluca et al., 2008). Increased warming at higher elevations has particular ecological importance in Hawaii, as the vast majority of remaining native forests in the state is found above 800 m elevation.

This highly controlled MAT gradient in tropical montane wet forests provides a space-for-time substitution study design that allowed us to examine the response of F_S to increasing MAT, with the specific objectives to quantify the magnitude of annual F_S, and plot-level spatial and diel variability in instantaneous F_S in response to increasing temperature. We hypothesized that: (*i*) the magnitude of annual F_S would increase with MAT, in line with prior studies (Bond-Lamberty and Thomson, 2010; Litton and Giardina, 2008; Rodeghiero and Cescatti, 2005); (*ii*) the plot-level spatial variability of instantaneous F_S would increase with MAT as a result of increased flux rates (Khomik et al., 2006); and (*iii*) the diel variability of instantaneous F_S would decrease with increasing MAT as a result of an anticipated decrease in diel fluctuations of soil temperature at warmer MATs. We tested these hypotheses by quantifying instantaneous F_S monthly for one year in a series of nine permanent plots arrayed across this 5.2 °C MAT gradient in Hawaiian tropical montane wet forests.

2. Methods

2.1. Study site

The study was conducted in a series of nine 20 × 20 m plots on the northeast slope of Mauna Kea Volcano, Island of Hawaii in the Hawaii Experimental Tropical Forest (HETF; 19°56′41.3″N, 155°15′44.2″W; 600–1800 m.a.s.l) of the USDA Forest Service, Pacific Southwest Research Station, and the Hakalau Forest National Wildlife Refuge (HFNWR; 19°50′31.3″N, 155°17′35.2″W; 600–2000 m.a.s.l) of the U.S. Fish and Wildlife Service. All plots are located in tropical montane wet forests and are classified as *Metrosideros polymorpha* Gaudich.–*Acacia koa* A. Gray forests. Across all plots, *M. polymorpha* (canopy tree species) and *Cheirodendron trigynum* (Gaudich.) A. Heller (midstory tree species) comprise 84–97% of stand basal area (BA) excluding tree ferns. Three species of tree ferns (*Cibotium* spp.) are also important constituents of the midstory, comprising an average of 46% (range 0–77%) of total stand BA. Overall, stand BA increases with MAT across the gradient, while stand density decreases with MAT (Table 1; see also Results and Discussion).

MAT across the gradient ranges from 13 °C at the top of HFNWR to 18.2 °C at the bottom of the HETF, while mean annual precipitation (MAP) varies from ~3200 at the top to ~4200 mm at the bottom of the gradient (Table 1). Because no site receives <3200 mm MAP and higher MAPs occur at higher MATs where evapotranspiration rates are higher, soil water balance is high and constant across the entire gradient (see Results).

Substrate in all plots is ~20 ky (14–65 ky) weathered tephra, and soils are moderate to well-drained hydrous, ferrihydritic/amorphic, isothermic/isomesic Acrudoxic Hydrudands of the Akaka, Honokaa, Maile, and Piihonua soil series (Table 2; Soil Survey Staff 2010). Across the gradient, soils are acidic (mean pH = 3.9), have high base saturation (mean = 32.4%) and estimated cation exchange capacity (mean = 11.9 cmol kg^{-1}), and average

Table 1
Environmental and stand characteristics of nine permanent plots along a 5.2 °C mean annual temperature gradient in tropical montane wet forests on the Island of Hawaii.

Plot & Elev. (m.a.s.l.)	MAT[a] (°C)	MAP[b] (mm)	Stand Density (individuals ha^{-1})	Stand Basal Area (m^2 ha^{-1})
SPE800	18.2	4204	4225	116
SPE934	17.3	4133	3300	100
SPE1024	16.7	4043	3750	97
SPE1116	16.1	3988	4275	155
WPL1116	16.1	3714	5875	109
WPL1204	15.5	3521	3900	102
WPL1274	15.1	3448	4375	81
HAK1468	13.8	3488	13,200	54
HAK1600	13.0	3195	16,400	66

[a] Mean annual temperature (MAT) calculated from a 30 y climate record (1961–1990) at the Hilo International Airport (8 m.a.s.l.) and the environmental lapse rate (6.49 °C 1000 m^{-1}).
[b] Mean annual precipitation (MAP) from Giambelluca et al. (1986).

Table 2
Soil properties of nine permanent plots along a 5.2 °C mean annual temperature gradient in tropical montane wet forests on the Island of Hawaii.

Plot & Elev. (m.a.s.l.)	Soil Series[a]	pH[b]	ECEC[b] (cmol kg^{-1})	Base Saturation[b] (%)	Bulk Density[c] (g cm^{-3})	C Content[c] (%)
SPE800	Akaka	4.1	9.3	57.8	0.21	9.7
SPE934	Akaka	4.2	9.6	37.8	0.19	15.7
SPE1024	Akaka	3.7	11.4	27.6	0.19	15.1
SPE1116	Akaka	3.8	16.4	27.7	0.20	15.3
WPL1116	Honokaa	3.6	15. 9	35.6	0.26	13.9
WPL1204	Honokaa	3.7	12.1	25.3	0.23	15.3
WPL1274	Maile	3.9	12.3	24.4	0.22	13.1
HAK1468	Akaka	4.2	8.5	27.1	0.18	15.4
HAK1600	Piihonua	4.1	11.3	27.9	0.23	12.6

[a] Soil in all plots classified as hydrous, ferrihydritic/amorphic, isothermic/isomesic Acrudoxic Hydrudands.
[b] pH, ECEC (estimated cation exchange capacity) and base saturation quantified on fresh soil samples (10 cores $plot^{-1}$) at field moisture collected to a depth of 10 cm.
[c] Bulk density and carbon content of <2 mm mineral soil to a depth of 91.5 cm (3–4 cores $plot^{-1}$).

bulk density and C content of 0.21 g cm^{-3} and 14.0%, respectively (Table 2).

Despite the environmental controls afforded by working in Hawaii highlighted above, a major source of uncertainty in all studies of ecosystem processes lies in the lack of information on disturbance history. Even in relatively intact forests such as the HETF and HFNWR, disturbance events ranging from gap-phase tree turnover on small scales to weather-related events on larger scales impart variability in forest structure that influences spatial and temporal variation in biogeochemical processes (Vitousek et al., 2010). To control for disturbance history effects across this MAT gradient, we used airborne light detection and ranging (LiDAR) measurements of forest structure to select seven sites in the HETF at each of six target elevations, where each site represents the maximum aboveground biomass present at a given elevation. The details of this methodology were reported by Asner et al. (2009), but are summarized here due to their importance to this study. LiDAR-based information at a 1.12 m resolution was acquired with the Carnegie Airborne Observatory (CAO; Asner et al., 2007) to quantify mean tree height across each elevation/MAT band specified on a single substrate type and age (~20 ky Acrudoxic Hydrudands). This was repeated for each of 6 elevation bands (two plots are located at the same elevation on opposite sides of the HETF for comparison). The CAO LiDAR was operated at 50 kHz, with a maximum half-scan angle of 17 (after 2-degree cutoff) degrees and 50% overlap between adjacent flight lines to ensure canopy penetration (Asner et al., 2008). The LiDAR point cloud data were analyzed using a physical model to derive surface (top-of-canopy) and ground digital elevation models (DEM), and vegetation height was estimated by differencing the surface and ground surface DEMs. Vertical errors in ground heights and vegetation heights were previously estimated to be 0.12 m (S.E. = 0.14 m) and 0.7 m (S.E. = 0.2 m), respectively (Asner et al., 2008, 2007).

Data for potential 20 × 20 m plots (with 1.12 × 1.12 m resolution pixel size) at each target elevation were assembled into mean canopy height maps that were visually inspected for candidate plots. Candidate plots were selected for field surveys if the plot met the criteria of sustaining mean canopy height that was within 10% of the maximum mean canopy height for a particular elevation band. An average of 10 plots per elevation band was visited for the six target elevations (seven sites) in the HETF. Selection of the final permanent plots was based on slope (<10° slope) and species composition (canopy dominated by living *M. polymorpha*). Because remote sensing information was not available for the two highest elevation HFNWR plots, we used traditional, intensive ground based survey techniques to replicate the remote sensing approach used in the HETF.

Subsequent remote sensing work on gap formation in this landscape (Kellner and Asner, 2009) revealed that the seven HETF plots all occur in moderately aggrading mature forests, indicating that overall site selection provided maximum potential biomass for a given elevation and controlled for disturbance history at each target MAT. As a result of this site selection procedure, and in line with previous findings for the larger landscape (Asner et al., 2009) and other tropical montane forests (Moser et al., 2011; Raich et al., 2006), stand BA increases with temperature along the gradient while stand density decreases (see Results). In total, nine 20 × 20 m plots (each subdivided into sixteen 5 × 5 m subplots) were established along a 5.2 °C MAT gradient, seven in the HETF at elevations ranging from 800 to 1274 m.a.s.l., and two in the HFNWR at 1468 and 1600 m.a.s.l. (Table 1).

2.2. Soil-surface CO_2 efflux

To quantify C flux from soils as F_S, 20 cm diameter and 12 cm tall PVC collars were inserted 6 cm into the soil (litter layer intact) at the center of each of eight 5 × 5 m subplots in all nine permanent plots along the MAT gradient in January and February of 2009. F_S and soil temperature (T_{SOIL}; 10 cm depth; one measurement per collar), and soil volumetric water content (VWC; top 12 cm; four measurements per collar) were measured monthly from May 2009 to April 2010 with a portable LI-8100 soil CO2 flux system and a 20 cm survey chamber (LI-COR, Lincoln, NE, USA) and a Hydrosense Soil Water Measurement System (Campbell Scientific, Inc., Logan, UT, USA), respectively. Annual F_S budgets were constructed for each plot from monthly instantaneous F_S measurements by multiplying mean monthly flux rates for each plot by the number of seconds in the day (there was no diel pattern in instantaneous F_S; see Results), scaling to g C m^{-2} day^{-1}, averaging daily rates over the 12 month study period, and multiplying by 365 days. All instantaneous F_S measurements were taken at least two months after collar installation to minimize associated disturbance effects. Final instantaneous F_S values for a given collar were calculated as the mean of two consecutive measurements with a 1 min delay between measurements. In cases where the first and second measurements varied by >15%, one or more additional measurements were taken to reduce variation to <15%. Sampling on all eight collars in a given plot during each month was completed within a 1 h period, and F_S in all plots across the gradient was measured each month over a three day period with constant weather conditions. All F_S measurements were screened for initial CO_2 concentration, and were eliminated from the dataset if initial CO_2 exceeded 450 ppm (a total of 14 out of 1728 measurements were discarded as a result, or 0.8% of the entire dataset). Zero and span gas (505 ppm) calibrations of CO_2 and zero gas calibration of H_2O were performed prior to each set of monthly flux measurements.

To assess plot-level spatial variability in instantaneous F_S, eight additional collars were added to the center of the remaining eight 5 × 5 m subplots in each of six plots along the MAT gradient (13.0, 13.8, 15.1, 16.1, 16.1 and 17.3 °C), and instantaneous F_S on all 16 collars within these plots was measured within a 2 h time period over seven days with constant weather conditions in late June and early July of 2009, a minimum of 72 h after collar installation. Spatial F_S measurements were conducted and screened following the protocol described above for monthly measurements.

For assessing plot-level diel variability in instantaneous F_S, a single collar was selected in each of three plots (13.0, 15.1, and 17.3 °C; Table 1) as the collar with the instantaneous F_S rate closest

to the plot mean value based on data from the spatial variability study described above. Diel F_S was measured in each plot with a LI-COR 8100 soil CO_2 flux system and an 8100-104 long-term chamber (LI-COR, Lincoln, NE, USA) every hour for 24 h. Diel F_S measurements were conducted and screened following the protocol described above for monthly measurements.

2.3. Data analysis

All statistical analyses were conducted in SigmaPlot 11.0 (Systat Software, Inc., San Jose, CA, USA) at $\alpha = 0.05$; where $\alpha > 0.05$ but <0.10, we identified the trend as marginally significant due to small sample sizes ($n = 6$ or 9). Linear regression analyses were used to: (*i*) quantify the influence of MAT, MAP, stand BA, stand density, and soil VWC on annual F_S; (*ii*) determine how the required sample size to estimate instantaneous F_S within 10 and 20% of the actual mean at the 95% probability level varied with MAT; and (*iii*) to examine the relationship between plot-level spatial and diel variability in instantaneous F_S and T_{SOIL}. In addition, power analyses of required sample sizes were computed in each of six plots with F_S data from 16 collars per plot. The sample size required for estimating F_S within 10 and 20% of the actual mean at a 95% probability level (Petersen and Calvin, 1986) was calculated as:

$$n = t_\alpha^2 s^2 / D^2 \quad (1)$$

where n is the required sample size, t_α is the Student's t statistic ($n - 1$ degrees of freedom = 15) at the 95% probability level, s is the standard deviation of plot-level F_S, and D is the desired confidence interval around the mean (10 or 20%).

3. Results

3.1. Magnitude of annual soil-surface CO_2 efflux in response to temperature

The annual flux of C from soil as F_S increased linearly with MAT ($r^2 = 0.72$; $P < 0.01$) at a rate of 141 g C m^{-2} y^{-1} for every 1 °C increase in MAT (Fig. 1; Table 3). The increase in annual F_S with MAT corresponded to a Q_{10} value of 2.26. Because MAP increased linearly with MAT along the gradient ($r^2 = 0.87$; $P < 0.01$), F_S also increased linearly with MAP ($r^2 = 0.63$; $P = 0.01$). However, because no site receives <3200 mm MAP, and higher MAPs occur at higher MATs where evapotranspiration rates are higher, soil volumetric water content did not vary with MAT ($r^2 = 0.00$; $P = 0.92$), averaging 52% (range 40–57%) across all plots over the 12 month measurement period (Table 3). As a result, annual F_S showed no relationship with mean annual soil volumetric water content along the MAT gradient ($r^2 = 0.00$; $P = 0.91$). Mean annual soil temperature at 10 cm was highly correlated with long-term estimated MAT across the gradient (Tables 1 and 3), differing on average by only ~0.5 °C ($T_{SOIL} = (1.02*MAT) - 0.45$; $r^2 = 0.99$; $P < 0.01$).

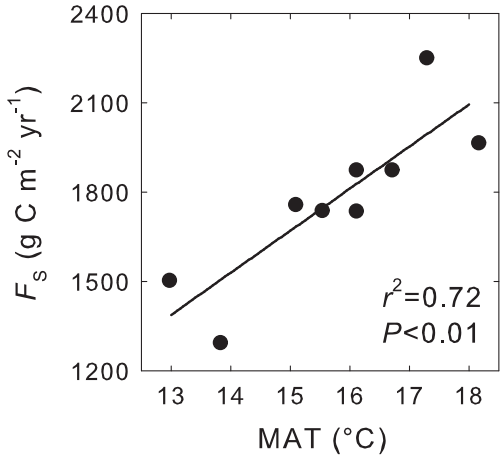

Fig. 1. Across a 5.2 °C mean annual temperature (MAT) gradient in Hawaiian tropical montane wet forests, annual soil-surface CO_2 efflux (F_S; g C m^{-2} y^{-1}) increased with MAT ($F_S = 141*MAT - 449$; $n = 9$; $r^2 = 0.72$; $P < 0.01$).

Table 3
Annual soil-surface CO_2 efflux (F_S; g C m^{-2} y^{-1}), mean annual soil temperature (T_{SOIL} at 10 cm; °C), and mean annual soil volumetric water content (VWC in top 12 cm; %) in nine permanent plots located along a 5.2 °C mean annual temperature gradient in Hawaiian tropical montane wet forests. All values were calculated from monthly measurements collected across one year in each plot.

Plot & Elev. (m.a.s.l.)	Annual F_S (g C m^{-2} y^{-1})	T_{SOIL} (°C)	Soil VWC (%)
SPE800	1953	18.0	55.3
SPE934	2234	17.3	54.8
SPE1024	1860	16.3	56.9
SPE1116	1860	15.9	48.0
WPL1116	1723	15.6	50.8
WPL1204	1726	15.5	40.2
WPL1274	1745	14.9	50.6
HAK1468	1285	13.6	55.3
HAK1600	1493	12.6	57.4

Strong seasonal patterns in daily F_S were apparent at all MATs, with a mean peak rate across all plots of 6.25 g C m^{-2} day^{-1} in August and a mean low rate across all plots of 3.63 g C m^{-2} day^{-1} in December (Fig. 2a). Seasonal patterns in T_{soil} were also clearly

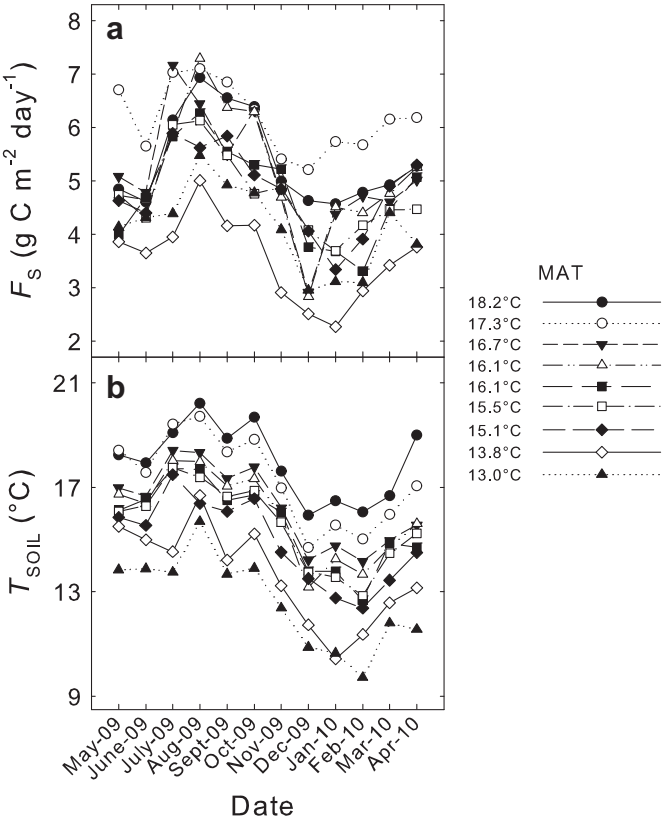

Fig. 2. Strong seasonal patterns in (a) daily soil-surface CO_2 efflux (F_S; g C m^{-2} day^{-1}) and (b) soil temperature (T_{SOIL}; °C at 10 cm depth) were evident for all nine plots across a 5.2 °C mean annual temperature (MAT) gradient in Hawaiian tropical montane wet forests. Seasonal patterns in F_S closely mirrored seasonal patterns in T_{SOIL}, with peak values in summer (July–September) and lowest values in winter (December–February). See Table 1 for site descriptions.

evident, and closely mirrored seasonal patterns in F_S (Fig. 2b). The strength of the monthly relationship between F_S and T_{soil} across the MAT gradient varied over time (r^2 ranged from 0.40 to 0.84; Mean = 0.63), but F_S increased linearly with T_{soil} for every monthly measurement period. There was no seasonal pattern in the strength of the relationship between T_{soil} and F_S for any MAT, or in the coefficient of variation (CV) of F_S. Likewise, no relationship existed between T_{soil} and the CV of F_S when data were pooled across all sites and months ($r^2 = 0.02$). Similarly, monthly Q_{10} values of F_S varied minimally over the year (Mean (±1 S.D.) = 2.31 (0.11)). Daily F_S was marginally correlated with soil VWC (r^2 of 0.38–0.40) during January, February and March of 2010, the only months when mean soil VWC across the gradient was ≤40%. Over the entire dataset, the strength of the relationship between F_S and soil VWC (i.e., r^2 value) decreased linearly, although marginally, with increasing soil VWC ($r^2 = 0.35$).

Across all plots, F_S increased linearly with stand BA ($r^2 = 0.38$; $P = 0.08$) and decreased linearly with stand density ($r^2 = 0.46$; $P = 0.05$) as a result of forest structural changes across the MAT gradient. Stand BA increased linearly with MAT ($r^2 = 0.43$; $P = 0.05$) and stand density decreased linearly with MAT ($r^2 = 0.71$; $P < 0.01$), such that stand density decreased linearly with stand BA ($r^2 = 0.71$; $P < 0.01$).

3.2. Spatial variability in instantaneous soil-surface CO_2 efflux and response to temperature

Both sampling approaches (8 versus 16 measurements per plot across 6 plots) yielded similar positive linear relationships between instantaneous F_S and T_{SOIL} across the gradient (Fig. 3), but the relationship between F_S and T_{SOIL} was stronger for 8 than 16 measurements (r^2 of 0.81 and 0.60, respectively). The slope of the equation line was also higher for 8 (0.53 ± 0.13) than 16 (0.38 ± 0.13) measurements per plot, but the equation line for 16 measurements per plot fell entirely within the ±95% C.I.s for the equation line based on 8 measurements per plot across the range of measured soil temperatures.

Across all nine plots (8 measurements per plot), the within-plot CV of instantaneous F_S ranged from 17 to 46%, with an average CV of 33% (Table 4). There was no relationship between the CV of instantaneous F_S and MAT ($r^2 = 0.01$; $P = 0.80$), suggesting that the

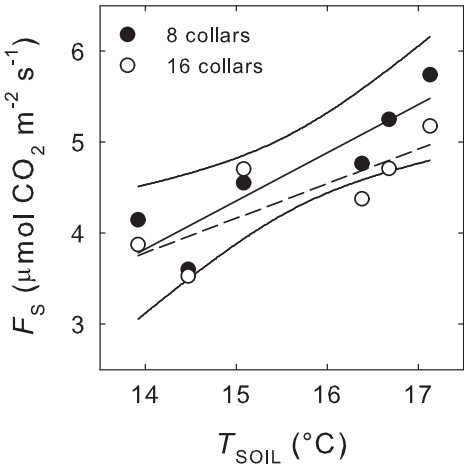

Fig. 3. The relationship between instantaneous soil-surface CO_2 efflux (F_S; µmol CO_2 m^{-2} s^{-1}) and soil temperature (T_{SOIL}; °C) was consistent when measurements were made at eight locations per plot (solid symbols and regression line ±95% C.I.s; FS = 0.53*T_{SOIL} − 3.58; $r^2 = 0.81$; $P = 0.01$) versus 16 locations per plot (open symbols and dashed regression line; $F_S = 0.34$*$T_{SOIL} - 0.92$; $r^2 = 0.60$; $P = 0.07$).

Table 4
Mean and coefficients of variation (CV; %) of instantaneous soil-surface CO_2 efflux (F_S; µmol CO_2 m^{-2} s^{-1}), soil temperature (T_{SOIL}; °C), and soil volumetric water content (VWC; %) along a 5.2 °C mean annual temperature gradient in Hawaiian tropical montane wet forests. Measurements were made in July 2009 once on 8 collars at each of nine plots (Spatial), or every h for 24 h on one collar in each of three plots (Diel).

Plot & Elev. (m)	Spatial			Diel	
	F_S	T_{SOIL}	VWC	F_S	T_{SOIL}
SPE800	4.45 (17.3)	17.9 (1.6)	70.1 (22.5)		
SPE934	5.44 (43.4)	17.1 (2.6)	54.0 (34.0)	7.7 (10.2)	18.6 (1.0)
SPE1024	4.59 (45.9)	16.7 (0.9)	68.4 (28.2)		
SPE1116	4.46 (36.1)	16.7 (1.7)	61.7 (28.7)		
WPL1116	4.51 (37.4)	16.4 (1.0)	52.7 (29.7)		
WPL1204	4.14 (22.3)	16.3 (2.1)	47.3 (24.4)		
WPL1274	4.23 (30.9)	15.1 (2.5)	48.3 (32.1)	4.2 (4.5)	15.7 (1.1)
HAK1468	3.51 (31.2)	14.5 (3.3)	52.9 (25.7)		
HAK1600	4.15 (30.2)	13.9 (1.5)	58.1 (30.0)	3.5 (4.9)	14.5 (0.4)

LiDAR process for plot selection was effective at controlling for variation in disturbance history while identifying potential sites with maximum biomass for a given MAT. Soil VWC also did not explain any spatial variation in instantaneous F_S, regardless of within-plot sample size.

Based on 16 measurements of instantaneous F_S per plot in six plots along the gradient, a power analysis quantified the need for relatively large sample sizes to estimate plot level instantaneous F_S within 10 and 20% of the actual mean at a 95% probability level. For $D = 10\%$, the required sample size ranged from 44 to 86 measurements per plot with a mean of 59, and for $D = 20\%$ the required sample size ranged from 11 to 21 measurements per plot with a mean of 15 (Table 5). Importantly, the required sample size increased linearly with MAT (Fig. 4), in contrast to the lack of a relationship between the CV of instantaneous F_S and MAT. While large sample sizes were identified for precise plot-level estimates of instantaneous F_S based on within-plot variability, a sampling scheme with only 8 measurements per plot was adequate for detecting strong significant relationships between F_S and T_{SOIL} across the MAT gradient (Fig. 3).

3.3. Diel variability in instantaneous soil-surface CO_2 efflux and response to temperature

When instantaneous F_S and T_{SOIL} were measured over 24 h (diel surveys) in three plots across the gradient (13.0, 15.1, and 17.3 °C), both increased with MAT, in line with the results presented above. Diel variability in instantaneous F_S increased with MAT (S.D. = 0.17, 0.19 and 0.78 µmol CO_2 m^{-2} s^{-1} at 13.0, 15.1, and 17.3 °C, respectively), as did diel variability in T_{SOIL} (S.D. = 0.06, 0.18 and 0.19 °C at 13.0, 15.1, and 17.3 °C, respectively). Positive linear relationships existed between instantaneous F_S and T_{SOIL} over a diel cycle at MATs of 17.3 °C ($n = 24$; $r^2 = 0.32$; $P < 0.01$) and 15.1 °C ($n = 24$; $r^2 = 0.18$; $P = 0.04$),

Table 5
Required sample sizes (n) for estimating plot-level soil-surface CO_2 efflux within 10 and 20% of the actual mean at the 95% probability level in six Hawaiian tropical montane wet forest plots. All analyses were based on instantaneous F_S measurements (µmol CO_2 m^{-2} s^{-1}) taken at 16 collars $plot^{-1}$.

Plot & Elev. (m)	n ($D = 10\%$)	n ($D = 20\%$)
SPE934	63	16
SPE1116	86	21
WPL1116	74	19
WPL1274	45	11
HAK1468	44	11
HAK1600	44	11

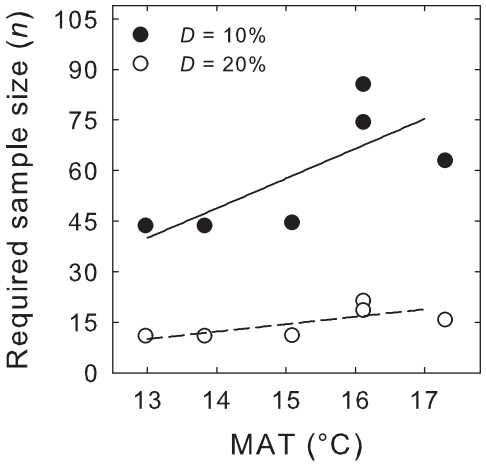

Fig. 4. The required sample size for estimating plot-level instantaneous soil-surface CO_2 efflux (F_S; μmol CO_2 m^{-2} s^{-1}) within 10% (solid symbols and line) and 20% (open symbols and dashed line) of the actual mean at a 95% probability level increased marginally with mean annual temperature (MAT) in Hawaiian tropical montane wet forests ($n = 6$; $r^2 = 0.52$; $P = 0.09$).

but not 13.0 °C ($n = 24$; $r^2 = 0.04$; $P = 0.33$). Despite significant relationships between instantaneous F_S and T_{SOIL}, diel variation in both variables was minimal within a given plot (Fig. 5). Across all three plots, T_{SOIL} varied by only 0.2–0.6 °C over 24 h. As a result, instantaneous F_S varied by an average of only 9% (range 3–17%) over 24 h. Critically, the CV for diel variability in instantaneous F_S, that is variation in instantaneous F_S over the course of a 24 h period (5%–10%, mean of 6.5%; Table 4), was small relative to the CV for spatial variability in instantaneous F_S within a plot (17%–46%, mean of 33%; Table 4).

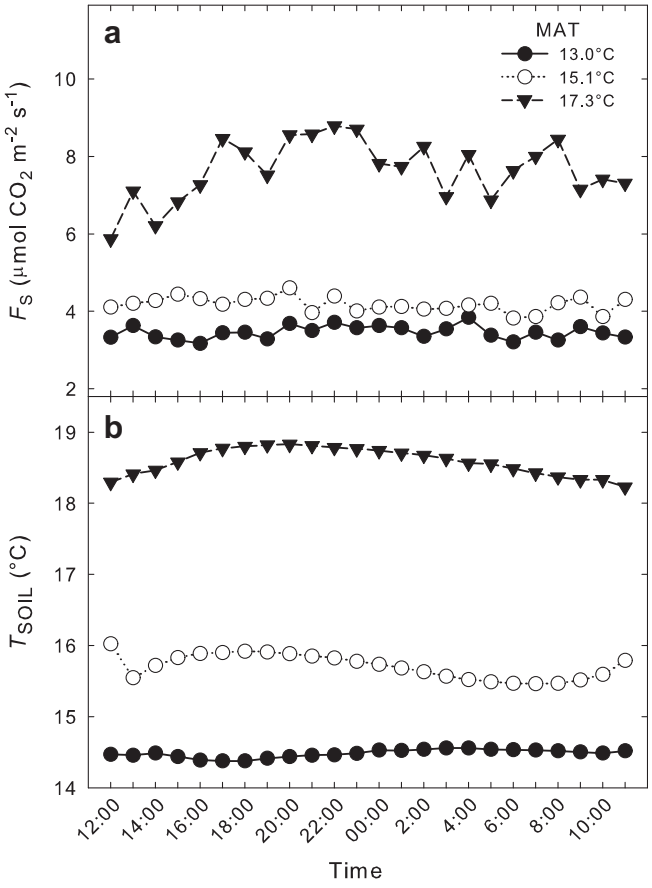

Fig. 5. Diel variability in instantaneous soil-surface CO_2 efflux (F_S; μmol CO_2 m^{-2} s^{-1}) and soil temperature (T_{SOIL}; °C at 10 cm depth) was minimal at three sites (13, 15.1 and 17.3 °C) along a 5.2 °C mean annual temperature gradient in Hawaiian tropical montane wet forests. See Table 1 for site descriptions.

4. Discussion

Quantifying how the magnitude of annual F_S, as well as spatial and temporal variation in instantaneous F_S, will respond to future warming is important to understanding how climate change will impact ecosystem C balance, including potential atmospheric feedbacks. In terrestrial ecosystems, spatial and temporal variability in F_S are influenced by numerous environmental factors, including temperature, moisture, photosynthetic activity, and disturbances (Ryan and Law, 2005; Vargas et al., 2011). However, it remains unclear how climate warming will impact the magnitude and variability in F_S at both instantaneous and annual scales. We utilized a highly controlled MAT gradient to evaluate both the magnitude of annual F_S and the spatial and diel variability in instantaneous F_S in response to MAT in Hawaiian tropical montane wet forests.

4.1. Magnitude of annual soil-surface CO_2 efflux in response to temperature

The annual F_S rates documented here (1295–2251 g C m^{-2} y^{-1} across the gradient) are in line with other tropical forest studies worldwide, including both intact lowland forests (1100–2280 g C m^{-2} y^{-1}; Davidson et al., 2002; Katayama et al., 2009; Litton et al., 2007; Salimon et al., 2004) and fast growing nonnative plantations (1920–2200 g C m^{-2} y^{-1}; Giardina and Ryan, 2002). In fact, the F_S rates documented here for warmer MAT plots are some of the highest reported to date for any forest ecosystem (Bahn et al., 2010; Hibbard et al., 2005; Katayama et al., 2009; Litton et al., 2007; Malhi et al., 2009), indicating that these forests are highly productive and on a par with wet forests in the lowland tropics.

Annual F_S was positively and linearly related to MAT, in line with our original hypothesis and prior studies (Bond-Lamberty and Thomson, 2010; Litton and Giardina, 2008; Rodeghiero and Cescatti, 2005), indicating that rising MAT will lead to higher annual fluxes of C to the atmosphere as F_S as long as ecosystem characteristics and functioning undergo concurrent changes as measured along this MAT gradient. While this trend is broadly appreciated in these prior studies, none have examined MAT effects under the highly controlled conditions of our gradient, where other sources of variation are largely controlled. The more than doubling of F_S with each 10 °C increase in MAT is also in line with previous analyses, but the precision of this increase across our MAT gradient ($Q_{10} = 2.26$) provides a more highly constrained estimate for modeling MAT effects on F_S in tropical montane wet forest ecosystems.

In this study, instantaneous F_S was measured monthly and integrated over one year to quantify the annual release of C from soil as F_S. While strong seasonal patterns were evident in daily F_S across the 12 month measurement period, and the seasonal pattern in F_S closely mirrored the seasonal pattern in T_{SOIL}, recent work highlighted that quantifying instantaneous F_S at mean annual temperature can be used to accurately predict annual F_S (Bahn et al., 2010). Utilizing this approach for our plots, instantaneous F_S measurements from November 2009 (the month with temperatures closest to long-term MAT values, with an average temperature difference across plots of 2.5%) resulted in annual F_S estimates that agreed well with our more detailed annual budgets ($r^2 = 0.74$

for measured versus predicted F_S, with a mean absolute difference of 6.9% across all nine sites). This highlights the utility of the Bahn et al. (2010) approach for quantifying large-scale patterns in annual F_S from one-time measurements conducted at a given site's MAT. Moreover, in this study similar patterns between MAT versus instantaneous F_S measured during any month of the year and MAT versus annual F_S highlights that one-time measurements can be valuable for identifying correlations with important environmental drivers of F_S.

Our findings are in line with previous studies documenting increased F_S with temperature at individual sites during the temperate zone winter to spring warm-up (Boone et al., 1998; Davidson et al., 1998), from *in-situ* warming studies (reviewed by Rustad et al., 2001), and across latitudinal (Janssens et al., 2001), elevational (Rodeghiero and Cescatti, 2005), and global MAT gradients (Litton and Giardina, 2008). Deciphering the mechanism responsible for increased F_S across studies is complicated by the fact that multiple C sources contribute to F_S, with alternative explanations for relationships between temperature and F_S having contrasting implications for terrestrial C balance. Further, each of these groups of studies likely captured different mechanisms driving increased F_S with temperature. For example, during winter to spring warm-up there is a large increase in the amount of photosynthate allocated belowground by trees as vernal changes also change conditions for canopy photosynthesis (Fitter et al., 1998; Högberg et al., 2002). Across latitude or elevation, it may be the length of the growing season that drives increasing productivity (Janssens et al., 2001), with increased productivity resulting in increased flux of autotrophic C to belowground (TBCF) (Litton and Giardina, 2008; Litton et al., 2007). Because annual F_S accounts for ~80% or more of the mass balance equation for estimating TBCF in forest ecosystems (Giardina and Ryan, 2002; Litton et al., 2004), increased annual F_S with MAT in this study is likely driven by a concurrent increase in stand productivity and the autotrophic flux of C to belowground with rising temperature, which has important but largely unexplored implications for the impacts of future warming on soil C pools (Bond-Lamberty and Thomson, 2010).

If increasing annual F_S with MAT results from MAT effects on ecosystem productivity, with increases in belowground productivity and TBCF driving higher F_S with warming, then soil C balance may be less sensitive to warming than currently predicted. However, if increasing MAT is driving an increase in heterotrophic use of soil C substrates and accelerated decomposition explains higher F_S, then warming may drive a reduction in soil C. Alternative interpretations also exist. For example, in soil warming studies (Luo et al., 2001; Melillo et al., 2002), F_S was initially stimulated by warming, but quickly "acclimated" and returned to baseline rates observed in control plots. This suggests that temperature increases can stimulate belowground metabolism, but in the absence of whole stand increases in productivity and TBCF, increases in F_S may not be sustained. This remains a crucial question in climate change science.

In this study, annual F_S was significantly correlated with stand BA, suggesting that for this gradient, increasing stand BA with MAT correlates with increased stand productivity, as seen in other tropical montane elevational gradients (Moser et al., 2011; Raich et al., 2006). Across our gradient, litterfall increased significantly with MAT (Freeman, Litton and Giardina, *Unpub. data*). Because litterfall is both an important component of F_S (Giardina et al., 2004; Raich and Nadelhoffer, 1989), and also a strong indicator of both net and gross primary productivity (Litton et al., 2007), the increase in F_S with MAT documented here likely reflects increased stand productivity with MAT. Again, the relationship between F_S and BA reflects the goal of the study design – to establish a MAT gradient where ecosystem processes are driven primarily by differences in temperature. The remote sensing approach used for plot selection was conducted such that plots were selected to represent the maximum biomass and, therefore, maximum BA at each elevation/MAT by controlling for disturbance history. As a result, we interpret variation in stand BA and stand density along the gradient as direct consequences of changes in MAT, and indirect drivers of changes in F_S. Declining stand density with MAT was driven primarily by the two coolest MAT sites where *Leptecophylla tameiameiae* (Cham. & Schltdl.) C. M. Weiller and *Vaccinium calycinum* Sm., small-statured understory trees/shrubs, were found in very high densities (average of 39% of all stems in these two plots) while being completely absent (*L. tameiameiae*) or in much lower densities (*V. calycinum*) in all other plots as a result of natural elevational distributions. Importantly, increasing stand density with decreasing MAT has also been documented for multiple other tropical elevation gradients (Alves et al., 2010; Culmsee et al., 2010; Moser et al., 2011).

Soil VWC was not related to annual F_S in this study because mean annual soil VWC varied minimally across the MAT gradient – again, the result of an appropriate study design and site-selection process prescribed to minimize variation in environmental factors other than MAT. Given larger variation in soil VWC, we would expect to find a stronger relationship with F_S and this was evident in monthly instantaneous F_S measurements, where the only months that showed a significant relationship between F_S and soil VWC were the three months when mean plot soil VWC was $\leq$40%. So while soil VWC was a very poor predictor of F_S on annual scales along this MAT gradient, instantaneous F_S was correlated with soil VWC when soils dried below some critical level. Given the importance of soil water availability in controlling F_S in more seasonally water-limited ecosystems (e.g., Litton et al., 2008), this is not surprising. However even in the three "dry" months in this study, MAT explained far more of the variability in F_S than soil VWC – again, highlighting the original intent and utility of this MAT gradient.

4.2. Spatial variability in instantaneous soil-surface CO_2 efflux and response to temperature

Across our gradient, instantaneous F_S was highly variable spatially, and this variability increased with increasing MAT, in line with our original hypothesis. Consequently, sample sizes required to estimate plot-level mean instantaneous F_S to a specified level of confidence increased with MAT. Prior studies have also documented increasing spatial variability in instantaneous F_S as both temperature and F_S increase across a growing season (Khomik et al., 2006). Notably, we found that doubling the sample size from 8 to 16 measurements within our 20 × 20 m plots did not yield significantly improved relationships between instantaneous F_S and temperature, with 8 collars reducing within-plot variability (i.e., S.E. of mean plot estimates) sufficiently to detect a strong, significant effect of MAT on F_S. To this end, our efforts to control for disturbance history and maximum potential biomass through airborne LiDAR-based plot selection reduced inter-plot variation in instantaneous F_S sufficiently to allow for detection of a significant effect of MAT on F_S across the gradient with only 8 measurements per plot.

Spatial variability in instantaneous F_S can be influenced by species composition (Fang et al., 1998; Hanson et al., 2000), structural attributes of the forest (Khomik et al., 2006), and soil properties such as moisture content (Adachi et al., 2005; Doff sotta et al., 2004) and fine root and microbial activity (Kuzyakov, 2006; Xu and Qi, 2001). In this study, MAP, T_{SOIL}, soil VWC, stand BA, and stand density were all examined as possible predictors of the spatial

variability in instantaneous F_S with increasing MAT. Of these, only T_{SOIL} exerted a significant influence on the spatial variability of instantaneous F_S, likely through temperature effects on litterfall rates, litter decomposition rates, TBCF, and fine root and microbial production. There is no kinetic or metabolic reason that we know of for increased temperature directly influencing the spatial variability of F_S. However, increased temperature likely influences the spatially variability of F_S by increasing the activity of the roots and microbes that produce CO_2 in soil to a greater extent than adjacent areas with limited roots and microbes.

Within plots, spatial variability in instantaneous F_S was marginally related to VWC at only the warmest MAT, indicating that as temperatures warm, increasing within-plot spatial variability in VWC may also drive increasing spatial variability in instantaneous F_S. While our goal was to understand spatial variability in instantaneous F_S within plots to better understand the effects of external factors on process rates across plots, future work should include structural and process studies to better understand the factors that regulate instantaneous F_S within plots.

4.3. Diel variability in instantaneous soil-surface CO_2 efflux and response to temperature

Efforts seeking to construct stand level C budgets are often challenged by the simultaneous need to reduce variation and minimize sample collection. For most ecosystems, especially those in the tropics, general guidelines do not exist for addressing diel variation in instantaneous F_S. However, prior studies have shown that diel variation in F_S is minimal for both native tropical dry forests (Litton et al., 2008) and tropical wet plantations (Giardina and Ryan, 2002) in Hawaii, and tropical forests elsewhere (Salimon et al., 2004). Low diel variability at all three MATs examined and the observation that daily F_S totals calculated from one-time instantaneous measurements and from diel sums were statistically indistinguishable, together, suggest that diel variation in tropical montane wet forests is a minor factor contributing to plot-level variability in instantaneous F_S. The lack of a diel pattern in instantaneous F_S is likely driven by minimal diel variation in the factors that most control F_S, including T_{SOIL} and soil VWC. For the Q_{10} of 2.26 found in this study describing the relationship between MAT and annual F_S, the narrow range observed in diel T_{SOIL} (0.2–0.6 °C) would have a very minor effect on temperature-dependent processes that drive F_S over a 24 h period.

Diel variability of instantaneous F_S and T_{SOIL} increased with MAT, in contrast to our original hypothesis. However, this diel variability was minor. Further, because the forest canopy at sites across this MAT gradient is tall (>25 m), the lags between photosynthesis and CO_2 released from the root rhizosphere and mycorrhizae may be several days (Kuzyakov and Gavrichkova, 2010). Importantly, these results indicate that instantaneous F_S measurements taken during any time of the day in tropical montane wet forests are adequate to accurately scale F_S to daily, monthly and annual ecosystem F_S budgets.

4.4. Conclusions

In conclusion, the results of this study indicate that with warming, annual F_S will increase and instantaneous F_S will become more spatially variable in tropical montane wet forests if ecosystem characteristics and functioning undergo concurrent changes as measured along this MAT gradient. This will thereby necessitate greater within-plot sampling effort. In line with other tropical forest studies, however, diel variation will remain a minor component of overall plot-level variation in instantaneous F_S. Increases in instantaneous and annual F_S with future warming warrant detailed attention in the context of potential changes in soil C pools and feedbacks to global climate change.

Acknowledgments

This study was funded by the National Science Foundation (Ecosystem Science Program; DEB-0816486); the USDA Forest Service, Institute of Pacific Islands Forestry, Pacific Southwest Research Station (Research Joint Venture 09-JV-11272177-029); and the College of Tropical Agriculture and Human Resources, University of Hawaii at Manoa (USDA CSREES HAW00132-H and HAW00188-M). Airborne data collection and analysis was funded by the Gordon and Betty Moore Foundation. The Carnegie Airborne Observatory is made possible by the W.M. Keck Foundation and William Hearst III. We thank the USDA Forest Service and State of Hawaii Department of Land and Natural Resources – Division of Forestry and Wildlife for access to the Hawaii Experimental Tropical Forest, and the U.S. Fish and Wildlife Service for access to the Hakalau Forest National Wildlife Refuge; Sharon Ziegler-Chong, Ulu Ching and Noelani Puniwai of the University of Hawaii at Hilo-Pacific Internship Program for Exploring Science (UH-PIPES) for logistical support; Darcey Iwashita, Rachel Moseley, Bernice Hwang, Cheyenne Perry, Jennifer Johansen, and Kevin Kaneshiro for field assistance; and Drs. Andy Taylor (University of Hawaii at Manoa) and Ken Gerow (University of Wyoming) for advice on data analyses. Two anonymous reviewers provided helpful comments during the review process.

References

Adachi, M., Bekku, Y.S., Konuma, A., Kadir, W.R., Okuda, T., Koizumi, H., 2005. Required sample size for estimating soil respiration rates in large areas of two tropical forests and of two types of plantation in Malaysia. Forest Ecology and Management 210, 455–459.

Alves, L.F., Vieira, S.A., Scaranello, M.A., Camargo, P.B., Santos, F.A.M., Joly, C.A., Martinelli, L.A., 2010. Forest structure and live aboveground biomass variation along an elevational gradient of tropical Atlantic moist forest (Brazil). Forest Ecology and Management 260, 679–691.

Asner, G.P., Knapp, D.E., Kennedy-Bowdoin, T., Jones, M.O., Martin, R.E., Boardman, J., Field, C.B., 2007. Carnegie Airborne Observatory: in-flight fusion of hyperspectral imaging and waveform light detection and ranging for three-dimensional studies of ecosystems. Journal of Applied Remote Sensing 1, 013521–013536.

Asner, G.P., Hughes, R.F., Vitousek, P.M., Knapp, D.E., Kennedy-Bowdoin, T., Boardman, J., Martin, R.E., Eastwood, M., Green, R.O., 2008. Invasive plants transform the three-dimensional structure of rain forests. Proceedings of the National Academy of Sciences 105, 4519–4523.

Asner, G.P., Hughes, R.F., Varga, T.A., Knapp, D.E., Kennedy-Bowdoin, T., 2009. Environmental and biotic controls over aboveground biomass throughout a tropical rain forest. Ecosystems 12, 261–278.

Bahn, M., Reichstein, M., Davidson, E.A., Grünzweig, J., Jung, M., Carbone, M.S., Epron, D., Misson, L., Nouvellon, Y., Roupsard, O., Savage, K., Trumbore, S.E., Gimeno, C., Curiel Yuste, J., Tang, J., Vargas, R., Janssens, I.A., 2010. Soil respiration at mean annual temperature predicts annual total across vegetation types and biomes. Biogeosciences 7, 2147–2157.

Bond-Lamberty, B., Thomson, A., 2010. Temperature-associated increases in the global soil respiration record. Nature 464, 579–582.

Boone, R.D., Nadelhoffer, K.J., Canary, J.D., Kaye, J.P., 1998. Roots exert a strong influence on the temperature sensitivity of soil respiration. Nature 396, 570–572.

Culmsee, H., Leuschner, C., Moser, G., Pitopang, R., 2010. Forest aboveground biomass along an elevational transect in Sulawesi, Indonesia, and the role of Fagaceae in tropical montane rain forests. Journal of Biogeography 37, 960–974.

Davidson, E., Belk, E., Boone, R., 1998. Soil water content and temperature as independent or confounding factors controlling soil respiration in a temperate mixed hardwood forest. Global Change Biology 4, 217–227.

Davidson, E.A., Savage, K., Bolstad, P., Clark, D.A., Curtis, P.S., Ellsworth, D.S., Hanson, P.J., Law, B.E., Luo, Y., Pregitzer, K.S., Randolph, J.C., Zak, D., 2002. Belowground carbon allocation in forests estimated from litterfall and IRGA-based soil respiration measurements. Agricultural and Forest Meteorology 113, 39–51.

Davidson, E.A., Janssens, I.A., Luo, Y., 2006. On the variability of respiration in terrestrial ecosystems: moving beyond Q_{10}. Global Change Biology 12, 154–164.

Doff sotta, E., Meir, P., Malhi, Y., Donato nobre, A., Hodnett, M., Grace, J., 2004. Soil CO_2 efflux in a tropical forest in the central Amazon. Global Change Biology 10, 601–617.

Fang, C., Moncrieff, J.B., Gholz, H.L., Clark, K.L., 1998. Soil CO_2 efflux and its spatial variation in a Florida slash pine plantation. Plant and Soil 205, 135–146.
Fitter, A.H., Graves, J.D., Self, G.K., Brown, T.K., Bogie, D.S., Taylor, K., 1998. Root production, turnover and respiration under two grassland types along an altitudinal gradient: influence of temperature and solar radiation. Oecologia 114, 20–30.
Giambelluca, T.W., Nullet, M.A., Schroeder, T.A., 1986. Rainfall Atlas of Hawaii. State of Hawaii. Department of Land and Natural Resources, Report R76, Honolulu, Hawaii, 267 pp.
Giambelluca, T.W., Diaz, H.F., Luke, M.S.A., 2008. Secular temperature changes in Hawaii. Geophysical Research Letters 35, L12702. doi:12710.11029/12008GL034377.
Giardina, C.P., Ryan, M.G., 2002. Total belowground carbon allocation in a fast growing *Eucalyptus* plantation estimated using a carbon balance approach. Ecosystems 5, 487–499.
Giardina, C.P., Binkley, D., Ryan, M.G., Fownes, J.H., Senock, R.S., 2004. Belowground carbon cycling in a humid tropical forest decreases with fertilization. Oecologia 139, 545–550.
Hanson, P.J., Edwards, N.T., Garten, C.T., Andrews, J.A., 2000. Separating root and soil microbial contributions to soil respiration: a review of methods and observations. Biogeochemistry 48, 115–146.
Hibbard, K.A., Law, B.E., Reichstein, M., Sulzman, J., 2005. An analysis of soil respiration across northern hemisphere temperate ecosystems. Biogeochemistry 73, 29–70.
Högberg, P., Nordgren, A., Ågren, G.I., 2002. Carbon allocation between tree root growth and root respiration in boreal pine forest. Oecologia 132, 579–581.
Janssens, I.A., Lankreijer, H., Matteucci, G., Kowalski, A.S., Buchmann, N., Epron, D., Pilegaard, K., Kutsch, W., Longdoz, B., Grunwald, T., Montagnani, L., Dore, S., Rebmann, C., Moors, E.J., Grelle, A., Rannik, U., Morgenstern, K., Oltchev, S., Clement, R., Gudmundsson, J., Minerbi, S., Berbigier, P., Ibrom, A., Moncrieff, J., Aubinet, M., Bernhofer, C., Jensen, N.O., Vesala, T., Granier, A., Schulze, E.D., Lindroth, A., Dolman, A.J., Jarvis, P.G., Ceulemans, R., Valentini, R., 2001. Productivity overshadows temperature in determining soil and ecosystem respiration across European forests. Global Change Biology 7, 269–278.
Katayama, A., Kume, T., Komatsu, H., Ohashi, M., Nakagawa, M., Yamashita, M., Otsuki, K., Suzuki, M., Kumagai, T.o, 2009. Effect of forest structure on the spatial variation in soil respiration in a Bornean tropical rainforest. Agricultural and Forest Meteorology 149, 1666–1673.
Kellner, J.R., Asner, G.P., 2009. Convergent structural responses of tropical forests to diverse disturbance regimes. Ecology Letters 12, 887–897.
Khomik, M., Arain, M.A., McCaughey, J.H., 2006. Temporal and spatial variability of soil respiration in a boreal mixedwood forest. Agricultural and Forest Meteorology 140, 244–256.
Khomik, M., Arain, M.A., Brodeur, J.J., Peichl, M., Restrepo-Coupé, N., McLaren, J.D., 2010. Relative contributions of soil, foliar, and woody tissue respiration to total ecosystem respiration in four pine forests of different ages. Journal of Geophysical Research 115, G03024. doi:03010.01029/02009JG001089.
Kuzyakov, Y., Gavrichkova, O., 2010. Time lag between photosynthesis and carbon dioxide efflux from soil: a review of mechanisms and controls. Global Change Biology 16, 3386–3406.
Kuzyakov, Y., 2006. Sources of CO_2 efflux from soil and review of partitioning methods. Soil Biology & Biochemistry 38, 425–448.
Law, B.E., Ryan, M.G., Anthoni, P.M., 1999. Seasonal and annual respiration of a ponderosa pine ecosystem. Global Change Biology 5, 169–182.
Litton, C.M., Giardina, C.P., 2008. Below-ground carbon flux and partitioning: global patterns and response to temperature. Functional Ecology 22, 941–954.
Litton, C.M., Ryan, M.G., Knight, D.H., 2004. Effects of tree density and stand age on carbon allocation patterns in postfire lodgepole pine. Ecological Applications 14, 460–475.
Litton, C.M., Raich, J.W., Ryan, M.G., 2007. Review: carbon allocation in forest ecosystems. Global Change Biology 13, 2089–2109.
Litton, C.M., Sandquist, D.R., Cordell, S., 2008. A non-native invasive grass increases soil carbon flux in a Hawaiian tropical dry forest. Global Change Biology 14, 726–739.
Luo, Y., Wan, S., Hui, D., Wallace, L., 2001. Acclimatization of soil respiration to warming in a tall grass prairie. Nature 413, 622–625.
Malhi, Y., Eduardo, L., Aragáo, O.C., Metcalfe, D.B., Paiva, R., Quesada, C.A., Almeida, S., Anderson, L., Brando, P., Chambers, J.Q., Costa, A.C.L.d., Hutyra, L.R., Oliveira, P., Patiño, S., Pyle, E.H., Robertson, A.L., Teixeira, L.M., 2009. Comprehensive assessment of carbon productivity, allocation and storage in three Amazonian forests. Global Change Biology 15, 1255–1274.
Melillo, J.M., Steudler, P.A., Aber, J.D., Newkirk, K., Lux, H., Bowles, F.P., Catricala, C., Magill, A., Ahrens, T., Morrisseau, S., 2002. Soil warming and carbon-cycle feedbacks to the climate system. Science 298, 2173–2176.
Moser, G., Leuschner, C., Hertel, D., Graefe, S., Soethe, N., Iost, S., 2011. Elevation effects on the carbon budget of tropical mountain forests (S Ecuador): the role of the belowground compartment. Global Change Biology 17, 2211–2226.
Petersen, R.G., Calvin, L.D., 1986. Sampling. In: Campbell, G.S., Nielsen, D.R., Jackson, R.D., Klute, C.A., Mortland, M.M. (Eds.), Methods of Soil Analysis. Part 1. Physical and mineralogical Methods. American Society of Agronomy, Inc. and Soil Science Society of America, Inc., Madison, WI, USA, pp. 33–51.
Raich, J.W., Nadelhoffer, K.J., 1989. Belowground carbon allocation in forest ecosystems: global trends. Ecology 70, 1346–1354.
Raich, J.W., Schlesinger, W.H., 1992. The global carbon dioxide flux in soil respiration and its relationship to vegetation and climate. Tellus Series B-Chemical and Physical Meteorology 44, 81–99.
Raich, J.W., Potter, C.S., Bhagawati, D., 2002. Interannual variability in global soil respiration, 1980–94. Global Change Biology 8, 800–812.
Raich, J.W., Russell, A.E., Kitayama, K., Parton, W.J., Vitousek, P.M., 2006. Temperature influences carbon accumulation in moist tropical forests. Ecology 87, 76–87.
Rodeghiero, M., Cescatti, A., 2005. Main determinants of forest soil respiration along an elevation/temperature gradient in the Italian Alps. Global Change Biology 11, 1024–1041.
Rodeghiero, M., Cescatti, A., 2008. Spatial variability and optimal sampling strategy of soil respiration. Forest Ecology and Management 255, 106–112.
Rustad, L., Campbell, J., Marion, G., Norby, R., Mitchell, M., Hartley, A., Cornelissen, J., Gurevitch, J., GCTE-News, 2001. A meta-analysis of the response of soil respiration, net nitrogen mineralization, and aboveground plant growth to experimental ecosystem warming. Oecologia 126, 543–562.
Ryan, M.G., Law, B.E., 2005. Interpreting, measuring, and modeling soil respiration. Biogeochemistry 73, 3–27.
Salimon, C.I., Davidson, E.A., Victoria, R.L., Melo, A.W.F., 2004. CO_2 flux from soil in pastures and forests in southwestern Amazonia. Global Change Biology 10, 833–843.
Stoyan, H., De-Polli, H., Böhm, S., Robertson, G., Paul, E., 2000. Spatial heterogeneity of soil respiration and related properties at the plant scale. Plant and Soil 222, 203–214.
Tang, J., Baldocchi, D.D., Xu, L., 2005. Tree photosynthesis modulates soil respiration on a diurnal time scale. Global Change Biology 11, 1298–1304.
Townsend, A.R., Vitousek, P.M., Trumbore, S.E., 1995. Soil organic matter dynamics along gradients in temperature and land use on the island of Hawaii. Ecology 76, 721–733.
Urbanski, S., Barford, C., Wofsy, S., Kucharik, C., Pyle, E., Budney, J., McKain, K., Fitzjarrald, D., Czikowsky, M., Munger, J.W., 2007. Factors controlling CO_2 exchange on timescales from hourly to decadal at Harvard Forest. Journal of Geophysical Research 112, G02020. doi:02010.01029/02006jg000293.
Vargas, R., Carbone, M., Reichstein, M., Baldocchi, D., 2011. Frontiers and challenges in soil respiration research: from measurements to model-data integration. Biogeochemistry 102, 1–13.
Vitousek, P.M., Tweiten, M.A., Kellner, J., Hotchkiss, S.C., Chadwick, O.A., Asner, G.P., 2010. Top-down analysis of forest structure and biogeochemistry across Hawaiian landscapes. Pacific Science 64, 359–366.
Vitousek, P.M., 2004. Nutrient Cycling and Limitation: Hawaii as a Model System. Princeton University Press, Princeton, New Jersey, 223 pp.
Xu, M., Qi, Y., 2001. Soil-surface CO_2 efflux and its spatial and temporal variations in a young ponderosa pine plantation in northern California. Global Change Biology 7, 667–677.
Zimmermann, M., Meir, P., Bird, M.I., Malhi, Y., Ccahuana, A.J.Q., 2010. Temporal variation and climate dependence of soil respiration and its components along a 3000 m altitudinal tropical forest gradient. Global Biogeochemical Cycles 24, GB4012. doi:4010.1029/2010GB003787.